Unique Curve for the Radiative Photovoltage Deficit Caused by the Urbach Tail

Juan Bisquert
Institute of Advanced Materials (INAM), Universitat Jaume I, 12006 Castelló, Spain

Email: bisquert@uji.es

Abstract

The photovoltage V_{oc} of high-performance solar cells such as GaAs and metal halide perovskites, is affected by the exponential Urbach tail in the absorption spectrum, with energy parameter E_U. It has been observed that increasing Urbach energy decreases the maximum photovoltage that can be achieved. Based on detailed balance and reciprocity of absorption and emission, we present a calculation that shows that the voltage loss due to the exponential tail in absorption obeys a universal relation $\Delta V_{oc}^{rad} = (k_B T/q)\ln(1 - E_U/k_B T)$ for $E_U < k_B T$, independently of the bandgap.

TOC

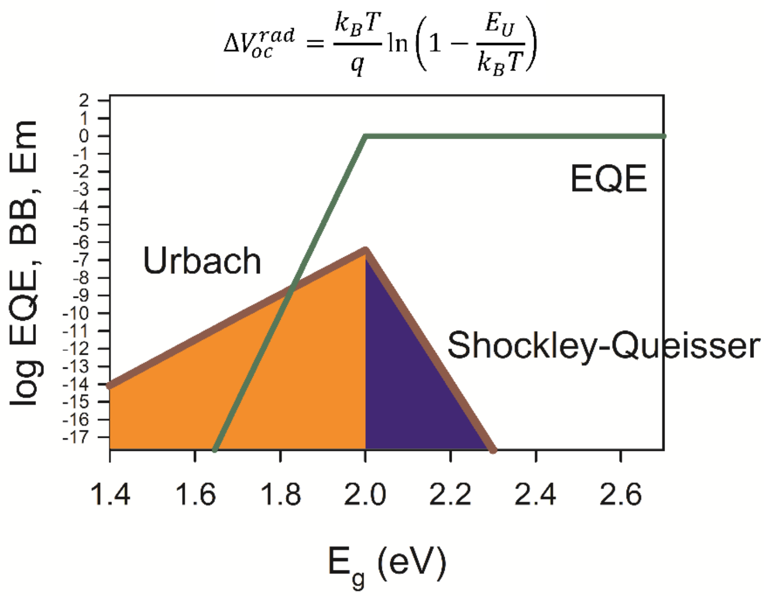

A calculation by detailed balance principle, first developed by Shockley and Queisser (SQ),[1] provides the reference of the maximum performance that solar cells can achieve in optimal conditions of operation.[2-4] In this method it is assumed that kinetic coefficients obtained in dark equilibrium can be applied in nonequilibrium conditions at high photon irradiation.[5,6] It is also assumed that recombination is given exclusively by the radiative recombination, hence the light absorption characteristic of the solar cell material is an essential feature to determine the corresponding performance.

The original detailed balance method[1] used a sharp absorption edge at the band gap energy E_g as the single parameter describing the semiconductor absorber. This type of absorption provides the standard limit open-circuit voltage V_{oc} as a function of the band gap, as shown in Fig. 1.[2,7] The voltage deficit is the difference of the energy of the generated electron-hole pair, to the energy at which it can be extracted at the contacts, $E_g/q - V_{oc}$,[6] where q is the electron charge. The operational loss is the voltage deficit at operation (maximum power) point.[4] It is shown in Fig. 1b and an updated version is presented in Ref. [8].

a) b)

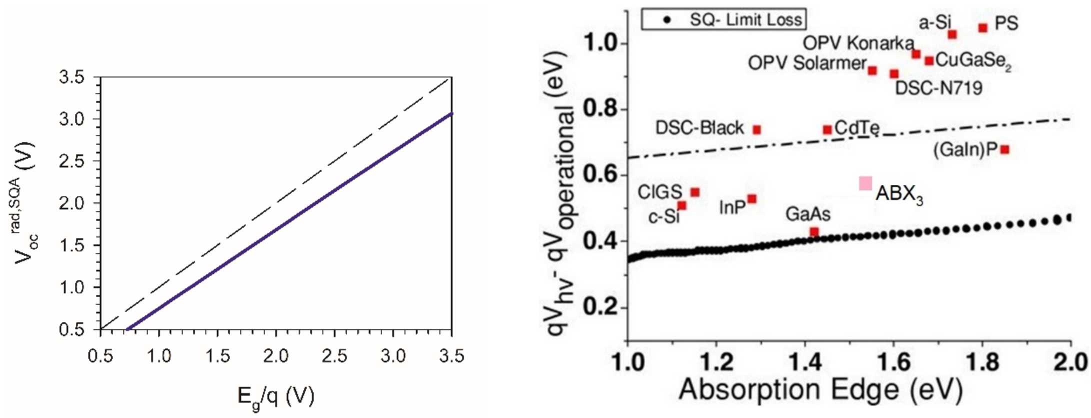

Fig. 1. a) The maximum photovoltage at one sun light intensity as a function of the bandgap according to detailed balance radiative limit with sharp absorption coefficient. The dashed line is $V_{oc} = E_g/q$. b) Experimental operational loss at maximum power versus E_g. The theoretical maximum loss (black circles) has been calculated in the SQ detailed balance limit. Reproduced with permission from [4].

While SQ is a useful benchmarking method, the photovoltaic outcome in real materials is affected by the fact that the density of states (DOS) and absorption coefficient are not an abruptly terminated step function. It is generally found by spectroscopy measurements that the density of states at the band edges and the optical absorption coefficient show a exponential shape termed the Urbach tail,[9,10] that is described by the following expression

$$\alpha(E) = \alpha_0 \exp\left(\frac{E-E_g}{E_U}\right) \qquad (E < E_g) \qquad (1)$$

α_0 is a material constant and E_U is a tailing parameter, associated to structural and thermal disorder.[11,12] An alternative expression for the absorption coefficient in a direct band gap semiconductor with an extent of disorder is a Gaussian distribution for the local band gap.[13-16] More generally a distribution function describes accurately the absorption edge.[8,17] Here we restrict our analysis to the implications of Eq. (1) for the gradual rise of the absorption edge.

Recently the influence of the Urbach tail on the conversion efficiency has been amply discussed for different photovoltaic technologies[8,18-20] and particularly for the metal halide perovskites.[21-23] The effect of the Urbach tail impacts mainly the voltage since the generation of current from the sub-bandgap levels is negligible. It is observed that the voltage deficit increases with increasing Urbach energy for a variety of technologies, as shown in Fig. 2[18] and in Ref. [8], see also [19,22].

This work aims to establish the physical limit to open circuit voltage with a realistic absorption model. We derive a general expression for evaluating the photovoltage loss in the radiative limit due to the absorption in the Urbach tail. For small $E_U < k_B T$ we obtain a universal curve valid for all classes of materials that depends only on E_U.

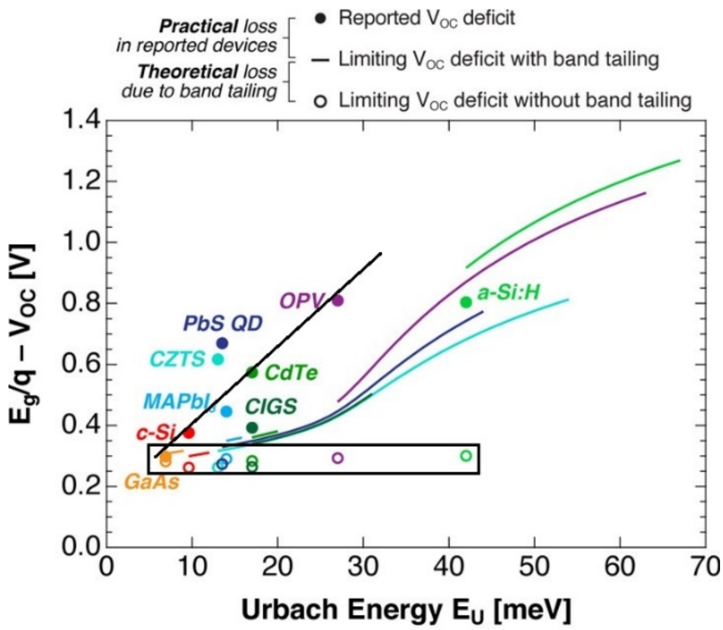

Fig. 2. The voltage deficit *vs* Urbach energy. Open circles indicate ideal detailed-balance limits without band tailing (E_U = 0). Solid lines represent the E_U range found in the literature and the corresponding range of detailed-balance limits. Filled circles indicate the performance of record-efficiency cells versus the lowest reported E_U values. Reproduced with permission from.[18] The square indicates the loss due to $V_{oc}^{rad,SQA}$ and the line indicates the points of measured V_{oc} deficit.

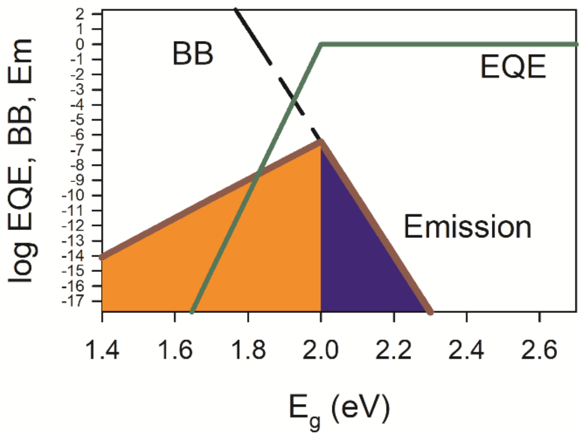

Fig. 3. Calculation of the emission from the photovoltaic EQE shown ($a_0 = 1$) and the blackbody radiation for a solar cell with an Urbach tail. The emission is given by the product of the two lines BB and EQE. The emission in Shockley-Queisser model is the blue area, while the additional emission due to the Urbach tail is the orange area.

Let us summarize the assumptions and the goals of our calculations. We apply the detailed balance method of radiative recombination to derive the fundamental maximum open circuit voltage in two cases. First, by standard Shockley-Queisser absorption model (SQA) we mean here a photovoltaic external quantum efficiency $EQE_{PV}(E) = 1$ for $E \geq E_g$ and 0 otherwise. As shown below the emission in SQA model is the blue triangle in Fig. 3. Second, we aim to derive the losses of V_{oc} that correspond to the sub-bandgap Urbach tail, the exponentially decaying part of EQE_{PV} below 2.0 eV in Fig. 3.

It must be remarked that there are different types of additional V_{oc} losses with respect to SQA model:

(1) The Urbach tail can form part of the radiative recombination model. By reciprocity of absorption and emission,[6] when adding the Urbach tail to SQA, we produce emission of radiation below E_g (the orange area in Fig. 3). This is the reason why the V_{oc} *decreases* with respect to SQA *even when all recombination is radiative.*

(2) There are other possible voltage losses, including nonradiative recombination states as well as the subunity efficiency of photon out-coupling.

In this paper we deal only with the effect of (1). We want to find the expressions that evaluate the excess loss of the radiative photovoltage introduced by the exponential tail of the DOS. Therefore, the target of our calculation is the quantity

$$\Delta V_{oc}^{rad} = V_{oc}^{rad} - V_{oc}^{rad,SQA} \tag{2}$$

where

(i) $V_{oc}^{rad,SQA}$ is the detailed balance limit for the photovoltage in SQA model, assuming a step function: $EQE_{PV}(E) = 1$ for $E \geq E_g$ and 0 otherwise.

(ii) V_{oc}^{rad} is the detailed balance limit for the photovoltage, assuming the Urbach tail in addition to SQA model.

The distinction of radiative (1) and other limitations (2) is an important element for the analysis of experiments: It must be separated the photovoltage loss due to radiative Urbach tail, that is given by the expressions derived below, and additional nonidealities in the particular device, that must be counted separately. Here we do not analyze the different causes for V_{oc} loss indicated in (2). This is a complex question depending on materials and technical details of devices. The loss of photovoltage beyond the radiative limit value is well described by the formula that includes EQE_{LED}, the emissive quantum yield[6,24]

$$V_{oc} - V_{oc}^{rad} = \frac{k_B T}{q} ln(EQE_{LED}) \quad (3)$$

k_B is Boltzmann's constant and T the absolute temperature. The quantity EQE_{LED} decreases at increasing factors of voltage loss (nonradiative recombination, outcoupling, etc.) and here we assume $EQE_{LED} = 1$.

We state the usual expressions of the detailed balance model that provide the physical limits to V_{oc} in a photovoltaic device.

In the dark at equilibrium the solar cell receives the blackbody radiation photon flux[6]

$$\phi_{ph}^{bb}(E) = b_\pi \frac{E^2}{e^{E/k_B T} - 1} \quad (4)$$

where $b_\pi = 2\pi/h^3c^2$ is a constant defined from Planck's constant h and the speed of light c. The spectral thermal emission ϕ_{ph}^{em} relates to the incoming radiation and the photovoltaic external quantum efficiency by the reciprocity expression[25,26]

$$\phi_{ph}^{em}(E) = EQE_{PV}(E)\phi_{ph}^{bb}(E) \quad (5)$$

At a certain applied voltage, V, Eq. (5) is extended as

$$\phi_{ph}^{em}(E, V) = EQE_{PV}(E)\phi_{ph}^{bb}(E)e^{qV/k_B T} \quad (6)$$

The main parameter determining recombination in a solar cell is the reverse saturation current j_0 of the diode model.[27] According to detailed balance method[1] the optimal performance of a solar cell is established by the radiative recombination current parameter, $j_{0,rad}$. It is given by the integral of the emission flux in equilibrium[6]

$$j_{0,rad} = q \int_0^\infty EQE_{PV}(E)\phi_{ph}^{bb}(E)dE \quad (7)$$

The radiative photovoltage is the open circuit voltage at 1 sun light intensity (corresponding to a photocurrent j_{ph}^{sun}) when all the nonradiative recombination channels are removed. It has the expression[6]

$$V_{oc}^{rad} = \frac{k_B T}{q} \ln\left(\frac{j_{ph}^{sun}}{j_{0,rad}}\right) \quad (8)$$

The calculation of V_{oc}^{rad} requires to first perform the integral in eq. (7) for the given model.

We now present the standard calculation of SQA model (as already said we have $EQE_{PV}(E) = 1$ for $E \geq E_g$ and 0 otherwise). The corresponding thermal emission is shown in Fig. 3 in the blue area. As there is no emission below E_g, the very low energies in Eq. (4) can be neglected as follows

$$\phi_{ph}^{bb}(E) = b_\pi E^2 e^{-E/k_B T} \quad (9)$$

and the integral of the emission in Eq. (7) is

$$j_{0,rad}^{SQA} = q b_\pi \int_{E_g}^{\infty} E^2 e^{-E/k_B T} dE =$$

$$= q b_\pi e^{-E_g/k_B T} k_B T \left({E_g}^2 + 2 E_g k_B T + 2 {k_B}^2 T^2\right) \quad (10)$$

Therefore

$$j_{0,rad}^{SQA} \approx q b_\pi e^{-E_g/k_B T} k_B T {E_g}^2 \quad (11)$$

Now we drop the SQA restriction of an abrupt absorption edge, and we use the Urbach tail absorption in Eq. (1). In general, we can write

$$EQE_{PV}(E) = a(E) IQE_{PV}(E) \quad (12)$$

in terms of the absorptivity a and the internal quantum efficiency. We assume perfect charge collection and hence $IQE_{PV} = 1$. For the absorptivity we must establish an optical model of the device. For example, for a solar cell of thickness d with antireflective coating and back mirror, using the Beer-Lambert expression, we obtain

$$a = 1 - e^{-2\alpha d} \quad (13)$$

We expect the tail absorption to be weak, therefore $a \approx 2\alpha d$. We define $a_0 = 2\alpha_0 d$ and we can write

$$EQE_{PV}(E) = a_0 \exp\left(\frac{E - E_g}{E_U}\right) \quad (14)$$

The EQE_{PV} is shown in Fig. 3. The area in orange in Fig. 3 is the additional emission with respect to SQA.

We start the calculation of ΔV_{oc}^{rad} first assuming $E_U < k_B T$ (later the general result for any E_U is discussed). This is a case of interest for high efficiency cells: Single-crystalline GaAs, Si, GaInP and InP, polycrystalline CdTe, metal halide perovskite, and CIGS, all have E_U values below $k_B T$.[8] In addition, the simplified expressions that are valid under this restriction illustrate well the physics of the model.

Owing to the additional absorption modes present with respect to SQA (orange area in Fig. 3), $j_{0,rad}$ increases and V_{oc}^{rad} decreases. From Eq. (7) we find

$$j_{0,rad} = j_{0,rad}^{SQA} + qb_\pi a_0 e^{-E_g/E_U} \int_0^{E_g} E^2 e^{(1/E_U - 1/k_B T)E} dE \tag{15}$$

Calculating the integral and neglecting small terms as in Eq. (11) the result takes the form

$$j_{0,rad} = \left(1 + \frac{a_0}{\frac{k_B T}{E_U} - 1}\right) j_{0,rad}^{SQA} \tag{16}$$

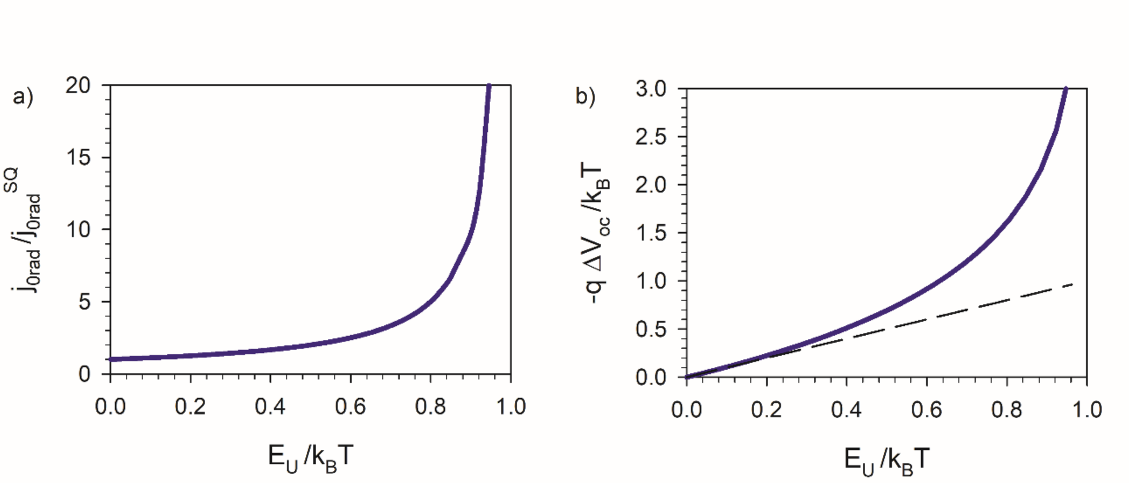

Fig. 4. (a) Excess radiative current due to the Urbach tail emission. (b) Universal curve for the radiative voltage deficit with respect to SQ value as a function of rescaled Urbach tail energy. The dashed line is the linear approximation. In both curves $a_0 = 1$.

The excess current is plotted in Fig. 4a. Inserting the value in Eq. (16) into Eq. (8) we obtain the expression for the voltage deficit in the radiative limit

$$\Delta V_{oc}^{rad} = V_{oc}^{rad} - V_{oc}^{rad,SQ} = -\frac{k_B T}{q} \ln\left[1 + \frac{a_0}{\frac{k_B T}{E_U} - 1}\right] \tag{17}$$

For a small value of a_0 it is a linear dependence

$$q\Delta V_{oc}^{rad} \approx -a_0 E_U \tag{18}$$

If we take $a_0 = 1$ in Eq. (17) to estimate large losses, we get

$$\Delta V_{oc}^{rad} = \frac{k_B T}{q} \ln\left(1 - \frac{E_U}{k_B T}\right) \tag{19}$$

The result is independent of E_g. The temperature can be rescaled as shown in Fig. 4b.

Hence the different photovoltaic technologies should obey a single universal curve.

In Fig. 5a the voltage loss (thick line) is shown at room temperature. Eq. (19) corresponds to the difference between filled and empty circles in Fig. 2. Note that the E_U values used in Fig. 2 are not necessarily the true E_U for the record cells.[18] For a quantitative analysis both the voltage deficit and E_U should be obtained for a unique cell.

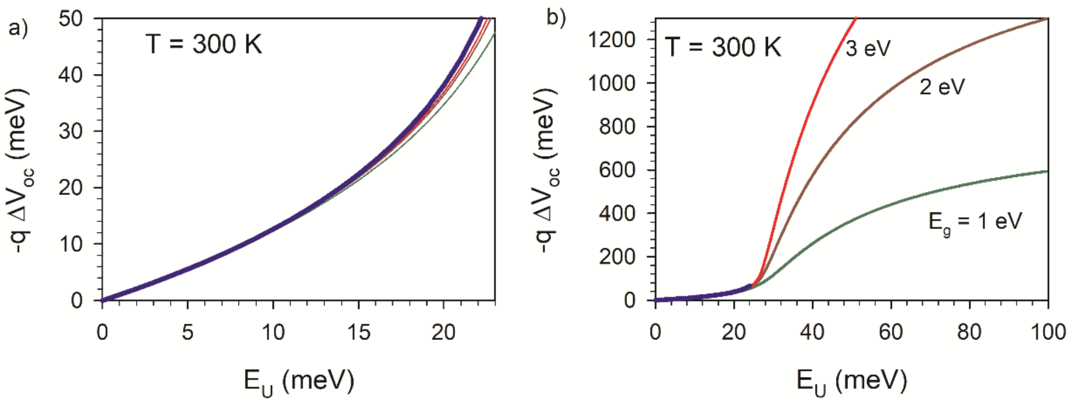

Fig. 5. The radiative voltage deficit $\Delta V_{oc}^{rad} = V_{oc}^{rad} - V_{oc}^{rad,SQA}$ (with respect to SQ value) as a function of Urbach tail energy for $a_0 = 1$. The thick blue line is the approximation at $E_U < k_B T$ and the thin lines are the general expression at different bandgap values. a) Small values of E_U. b) general range of E_U.

We now derive a general expression valid also when $E_U > k_B T$. For a-Si, CZTS, and organic solar cells, the E_U values are > 40 meV, with large impact on the voltage efficiency.[8] In this case the low energy part of the Planck formula (4) cannot be neglected. Eq. (15) is expressed as

$$j_{0,rad} = j_{0,rad}^{SQA} + q b_\pi a_0 e^{-E_g/E_U} \int_0^{E_g} \frac{E^2 e^{E/E_U}}{e^{E/k_B T} - 1} dE \tag{20}$$

We obtain

$$j_{0,rad} = j_{0,rad}^{SQA} \left(1 + a_0 \frac{e^{(1/k_B T - 1/E_U) E_g}}{k_B T {E_g}^2} I(E_U) \right) \tag{21}$$

and the general expression of the additional voltage loss with respect to SQ is

$$\Delta V_{oc}^{rad} = -\frac{k_B T}{q} \ln \left(1 + a_0 \frac{e^{(1/k_B T - 1/E_U) E_g}}{k_B T {E_g}^2} I(E_U) \right)$$

(22)

where the integral is

$$I_1(E_U) = \int_0^{E_g} \frac{E^2 e^{E/E_U}}{e^{E/k_BT} - 1} dE$$

(23)

The graphical representation of the expression, including large values of E_U, is obtained by numerical integration and it is shown in Fig. 5b. At $E_U > k_BT$ the lines of different E_g values depart from the unified curve.

Some limitations of detailed balance need to be carefully analyzed. A tailing of the DOS in the band gap introduces different possibilities of recombination events that affects the reciprocity formula (5) used in the above derivation.[28] The open circuit voltage under illumination in Eq. (8) has been obtained by the usual extrapolation involving detailed balance. It is assumed that the kinetic coefficients in equilibrium remain valid far from equilibrium in conditions of intense photoluminescence, e.g., by passing from Eq. (4) to Eq. (5).[6] It was explained by Cuevas that detailed balance between generation and recombination in equilibrium does not always apply to non-equilibrium situations, since the recombination parameter $j_{0,rad}$ may become a function of the concentration.[27]

Additionally, the occupation of the bands may modify the rate of absorption and recombination processes.[29] If a semiconductor works far from dark equilibrium but achieves equilibrium with an ensemble of thermalized photons, the Eq. (4) needs to be stated more generally as[6]

$$\phi_{ph}^{bb}(E, \Delta\mu) = b_\pi \frac{E^2}{e^{(E-\Delta\mu)/k_BT} - 1}$$

(24)

This equation has been obtained by Lasher and Stern[30] considering a population of photons at nonzero chemical potential $\Delta\mu$,[31,32] in equilibrium with the electrons and holes in a semiconductor with a splitting of Fermi levels $\Delta\mu$. Eq. (24) was extended by Würfel[33] for the external radiative emission from a semiconductor surface, leading to

$$\phi_{ph}^{em}(E, \Delta\mu) = b_\pi a(E) \frac{E^2}{e^{(E-\Delta\mu)/k_BT} - 1}$$

(25)

At open circuit conditions $\Delta\mu = qV_{oc}$. For $\Delta\mu \ll E_g$ we obtain from Eq. (25) the results in Eq. (6) and (8). If the DOS below the band gap is negligible (SQA model) the sub bandgap occupation need not be considered in detailed balance calculations. But in our analysis of $j_{0,rad}$ involving the Urbach tail in Eq. (20) we clearly integrate the sub-bandgap radiation modes. Hence, we pass through the singularity of Eq. (24) at $E = \Delta\mu$. This is due to the infinite occupation of the lowest available state in the Bose-Einstein distribution, and to the fact that energy levels are full below the electron Fermi level, and vice versa for the holes, so that absorption is not possible at $E < \Delta\mu$. These facts, that become more significant when the Fermi levels approach the band edges at high irradiation levels (leading to lasing at $\Delta\mu > E_g$), were first discussed by Parrott[34] introducing an occupation factor of the type

$$\alpha'^{(E,\Delta\mu)} = \tanh\left(\frac{E-\Delta\mu}{4k_BT}\right)\alpha(E) \tag{26}$$

that makes the absorption coefficient vanish at $E = \Delta\mu$, see the recent discussion by Wong et al.[20] Therefore one obtains

$$\phi_{ph}^{em}(E,\Delta\mu) = b_\pi a(E)E^2 \frac{\tanh\left(\frac{E-\Delta\mu}{4k_BT}\right)}{e^{(E-\Delta\mu)/k_BT}-1} \tag{27}$$

To analyze the modifications introduced by Eq. (26) in the Urbach tail absorption we can use the following form of EQE_{PV}

$$EQE_{PV}(E,\Delta\mu) = a_0 \exp\left(\frac{E-E_g}{E_U}\right)\tanh\left(\frac{E-\Delta\mu}{4k_BT}\right) \tag{28}$$

The emitted radiation is the product of Eqs. (24) and (28). The radiative recombination current parameter and voltage have the same expression as (21) and (22) respectively, but the integral is defined as

$$I_2(E_U,\Delta\mu) = \int_{\Delta\mu}^{E_g} \frac{E^2 e^{E/E_U}}{e^{(E-\Delta\mu)/k_BT}-1}\tanh\left(\frac{E-\Delta\mu}{4k_BT}\right)dE \tag{29}$$

Fig. 6 shows the change of the standard expressions when considering the effect of the finite chemical potential of light and electrons and holes. It is observed that the modified expressions change the dependence near $E \approx \Delta\mu$, and of course they create a cut-off to the exponential tails when going to lower energies. Fig. 7 shows the calculation of the effect of the occupancy of the DOS. The blue lines are the calculations shown before without the effect of the filling of states, only amplified by the voltage factor as in Eq. (6). The coloured lines are obtained from Eq. (22) with the integral (29). At low values of E_U the EQE_{PV} decreases sharply and the occupancy of deep states makes no effect, so that the universal formula (17) continues to hold true. When E_U increases the DOS goes deeper into the gap. The occupancy suppresses the radiative effect of the deep states, and the radiative voltage loss decreases. The more disordered solar cell materials will have an advantage in this respect, since the occupancy removes part of the V_{oc} losses caused by the Urbach tail.

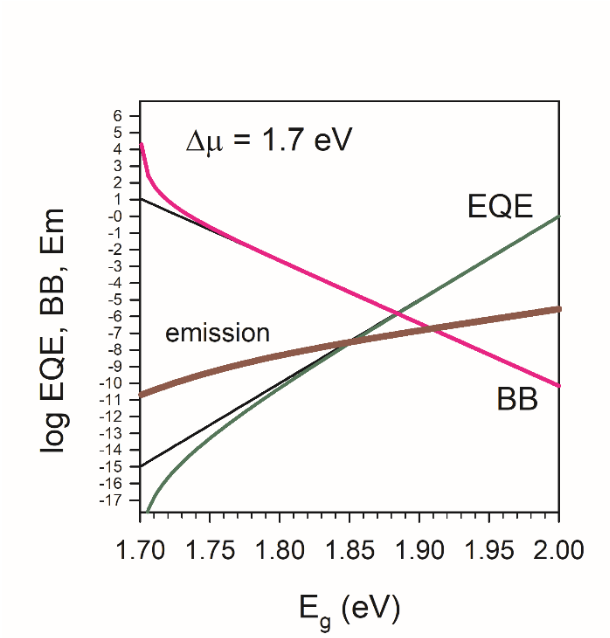

Fig. 6. For a semiconductor of $E_g = 2$ eV operating at a chemical potential $\Delta\mu = 1.7$ eV, it is shown the effective EQE_{PV}, the blackbody spectrum emission and the semiconductor light emission. The black lines are the reference for $\Delta\mu = 0$.

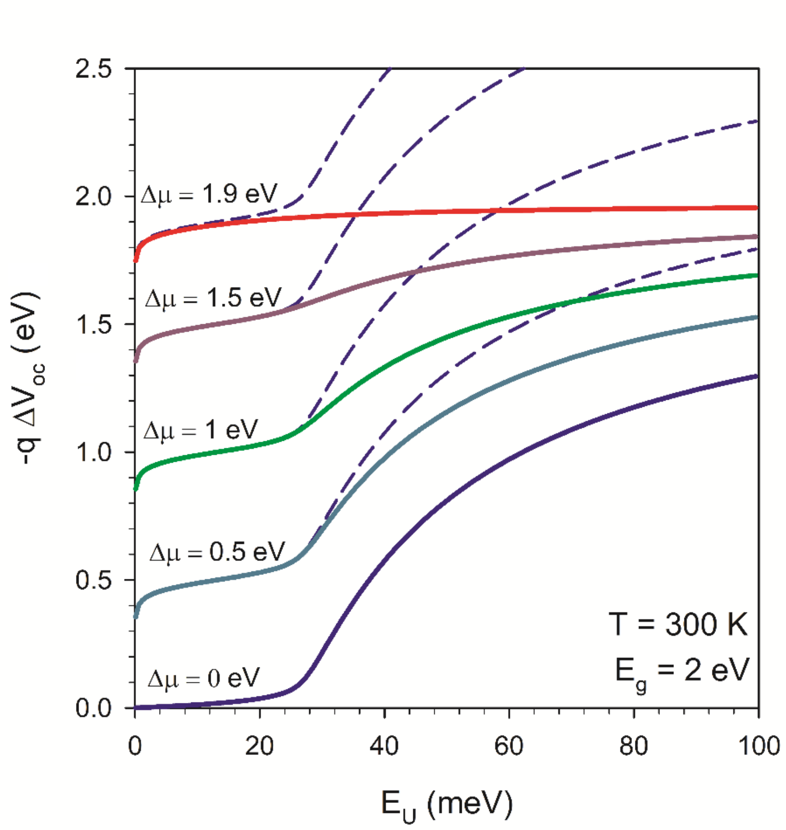

Fig. 7. The radiative voltage deficit $\Delta V_{oc}^{rad} = V_{oc}^{rad} - V_{oc}^{rad,SQ}$ (with respect to SQ value) as a function of Urbach tail energy for $E_g = 2$ eV and $a_0 = 1$, at different values

of the chemical potential $\Delta\mu$. Calculation by Eq. (22), the blue dashed line is for $I = I_1(E_U)e^{\Delta\mu/k_BT}$ and the colored lines are for $I_2(E_U, \Delta\mu)$.

In conclusion, we have discussed the maximum theoretical open-circuit voltage that can be obtained in a solar cell using a detailed balance method. We showed that a simple integration of the product EQE_{PV} times the blackbody radiation provides a universal formula of the voltage loss due to the Urbach tail in the radiative recombination limit, with respect to the Shockley-Queisser, abrupt absorption, model. A more general analysis based on a numerical integration describes the voltage loss for large values of the Urbach tail energy. The effect of the electrons and holes occupying the states of the semiconductor reduces the voltage losses when the exponential tail goes deep into the energy gap.

Acknowledgments

I thank the financial support by Ministerio de Ciencia y Innovación (PID2019-107348GB-100).

References

(1) Shockley, W.; Queisser, H. J. Detailed balance limit of efficiency of p-n junction solar cells, *J. Appl. Phys.* **1961**, *32*, 510-520.

(2) Hirst, L. C.; Ekins-Daukes, N. J. Fundamental losses in solar cells, *Prog. Photov.: Res. Appl.* **2011**, *19*, 286-293.

(3) Polman, A.; Knight, M.; Garnett, E. C.; Ehrler, B.; Sinke, W. C. Photovoltaic materials: Present efficiencies and future challenges, *Science* **2016**, *352*, aad4424.

(4) Nayak, P. K.; Bisquert, J.; Cahen, D. Assessing Possibilities and Limits for Solar Cells, *Adv. Mater.* **2011**, *23*, 2870-2876.

(5) Shockley, W.; Read, W. T. Statistics of the recombinations of holes and electrons, *Phys. Rev.* **1952**, *87*, 835-842.

(6) Bisquert, J. *The Physics of Solar Energy Conversion*; CRC Press: Boca Raton, 2020.

(7) Rühle, S. Tabulated values of the Shockley–Queisser limit for single junction solar cells, *Sol. Ener.* **2016**, *130*, 139-147.

(8) Nayak, P. K.; Mahesh, S.; Snaith, H. J.; Cahen, D. Photovoltaic solar cell technologies: analysing the state of the art, *Nat. rev. Mater.* **2019**, *4*, 269-285.

(9) Urbach, F. The long-wavelength edge of photographic sensitivity and of the electronic absorption of solids, *Phys. Rev.* **1953**, *92*, 1324-1324.

(10) Miller, O. D.; Yablonovitch, E.; Kurtz, S. R. Strong internal and external fluorescence as solar cells approach the Shockley-Queisser limit, *IEEE J. Photov.* **2012**, *2*, 303-311.

(11) John, S.; Soukoulis, C.; Cohen, M. H.; Economou, E. N. Theory of Electron Band Tails and the Urbach Optical-Absorption Edge, *Phys. Rev. Lett.* **1986**, *57*, 1777-1780.

(12) Studenyak, I.; Kranjec, M.; Kurik, M. Urbach Rule in Solid State Physics, *Int. J. Opt. Appl.* **2014**, *4*, 76-83.

(13) Mattheis, J.; Rau, U.; Werner, J. H. Light absorption and emission in semiconductors with band gap fluctuations---A study on Cu(In,Ga)Se2 thin films, *J. Appl. Phys.* **2007**, *101*, 113519.

(14) Gokmen, T.; Gunawan, O.; Todorov, T. K.; Mitzi, D. B. Band tailing and efficiency limitation in kesterite solar cells, *App. Phys. Lett.* **2013**, *103*, 103506.

(15) Kirchartz, T.; Taretto, K.; Rau, U. Efficiency Limits of Organic Bulk Heterojunction Solar Cells, *J. Phys. Chem. C* **2009**, *113*, 17958-17966.

(16) Katahara, J. K.; Hillhouse, H. W. Quasi-Fermi level splitting and sub-bandgap absorptivity from semiconductor photoluminescence, *J. Appl. Phys.* **2014**, *116*,

173504.

(17) Rau, U.; Blank, B.; Müller, T. C. M.; Kirchartz, T. Efficiency Potential of Photovoltaic Materials and Devices Unveiled by Detailed-Balance Analysis, *Phys. Rev. Appl.* **2017**, *7*, 044016.

(18) Jean, J.; Mahony, T. S.; Bozyigit, D.; Sponseller, M.; Holovský, J.; Bawendi, M. G.; Bulović, V. Radiative Efficiency Limit with Band Tailing Exceeds 30% for Quantum Dot Solar Cells, *ACS Energy Lett.* **2017**, *2*, 2616-2624.

(19) Michelle, S.; Alison, J. New Research in Solar Cells: Urbach Tails and Open Circuit Voltage, *Elements* **2015**, *11*.

(20) Wong, J.; Omelchenko, S. T.; Atwater, H. A. Impact of Semiconductor Band Tails and Band Filling on Photovoltaic Efficiency Limits, *ACS Energy Lett.* **2021**, *6*, 52-57.

(21) Ledinsky, M.; Schönfeldová, T.; Holovsky, J.; Aydin, E.; Hájková, Z.; Landová, L.; Neykova, N.; Fejfar, A.; De Wolf, S. Temperature Dependence of the Urbach Energy in Lead Iodide Perovskites, *J. Phys. Chem. Lett.* **2019**, *10*, 1368-1373.

(22) De Wolf, S.; Holovsky, J.; Moon, S.-J.; Löper, P.; Niesen, B.; Ledinsky, M.; Haug, F.-J.; Yum, J.-H.; Ballif, C. Organometallic Halide Perovskites: Sharp Optical Absorption Edge and Its Relation to Photovoltaic Performance, *J. Phys. Chem. Lett.* **2014**, *5*, 1035-1039.

(23) Ledinský, M.; Vlk, A.; Schönfeldová, T.; Holovský, J.; Aydin, E.; Dang, H. X.; Hájková, Z.; Landová, L.; Valenta, J.; Fejfar, A.; De Wolf, S. Impact of Cation Multiplicity on Halide Perovskite Defect Densities and Solar Cell Voltages, *J. Phys. Chem. C* **2020**, *124*, 27333-27339.

(24) Rose, A. L. Photovoltaic effect derived from the Carnot cycle, *J. Appl. Phys.* **1960**, *31*, 1640-1641.

(25) Rau, U. Reciprocity relation between photovoltaic quantum efficiency and electroluminescent emission of solar cells, *Phys. Rev. B* **2007**, *76*, 085303.

(26) Kirchartz, T.; Rau, U. Detailed balance and reciprocity in solar cells, *Phys. Stat. Solid. (a)* **2009**, *205*, 2737–2751.

(27) Cuevas, A. The Recombination Parameter J0, *Energy Procedia* **2014**, *55*, 53-62.

(28) Müller, T. C. M.; Pieters, B. E.; Kirchartz, T.; Carius, R.; Rau, U. Effect of localized states on the reciprocity between quantum efficiency and electroluminescence in Cu(In,Ga)Se2 and Si thin-film solar cells, *Sol. En. Mater. Sol. Cell* **2014**, *129*, 95-103.

(29) I thank Thomas Kirchartz for pointing out this problem.

(30) Lasher, G.; Stern, F. Spontaneous and Stimulated Recombination Radiation in Semiconductors, *Phys. Rev.* **1964**, *133*, A553-A563.

(31) Landsberg, P. T. Photons at non-zero chemical potential, *J. Phys. C* **1981**, *14*, L1025.

(32) Ries, H.; McEvoy, A. J. Chemical potential and temperature of light, *J. Photochem Photobiol. A: Chem.* **1991**, *59*, 11-18.

(33) Würfel, P. The chemical potential of radiation, *J. Phys. C* **1982**, *15*, 3967-3985.

(34) Parrott, J. E. Self-consistent detailed balance treatment of the solar cell, *IEE Proc.* **1986**, *133*, 314-317.